

ASSERT VALIDATION AGAINST THE STERN LABORATORIES' SINGLE-PHASE PRESSURE DROP TESTS

G. M. Waddington, J. C. Kiteley and M. B. Carver

AECL, Chalk River Laboratories, Fuel Channel Thermalhydraulics Branch
Chalk River, Ontario, CANADA K0J 1J0

Abstract

This paper describes the preliminary validation of ASSERT-IV against the single-phase pressure drop tests from the 37-element CHF experiments conducted at Stern Laboratories, and shows how this study fits into the overall ASSERT validation plan. The effects on the pressure drop of several friction and form loss models are evaluated, including the geometry-based K-factor model. The choice of friction factor has a small effect on the predicted channel pressure drop, compared to the form loss model choice. Using the uniform K-factors of Hameed, the computed pressure drops are in excellent agreement with the experimental results from the nominal pressure tube tests. For future ASSERT applications, either Hameed's uniform K-factors or the geometry-based model using Idelchik's thick-edged orifice equation are recommended, as are the friction factor correlations of Colebrook-White, Selander, and Aly and Groeneveld. More analysis of the geometry-based K-factor model is required.

1. Introduction

The ASSERT[†] subchannel analysis code^{1,2} models transient or steady-state, single- or two-phase flow and heat transfer in rod-bundle fuel channels. Since the ASSERT program is under continuous development, it requires continuous validation against relevant experimental data in order to evaluate any new models or code modifications.

Stern Laboratories' 37-element critical heat flux (CHF) experiments³ provide considerable data suitable for validating many components of the ASSERT code. In this study, the friction and form loss models are evaluated in comparison with the single-phase pressure drop data. Following this, the ASSERT validation plan calls for the evaluation of the two-phase multipliers against the two-phase pressure drop data; the effect of bundle orientation and pressure tube (PT) creep on the onset-of-dryout power will be compared to the initial dryout tests, and the onset-of-significant void (OSV) will be evaluated through comparison with the rod-wall temperature data from the profile scan tests.

The purpose of this study is to evaluate the friction and form loss models in ASSERT, and to recommend the best combination to use in later validation studies and other ASSERT applications. The effects of the friction factor and K-factor models on the pressure drop are examined and compared to data from the Stern single-phase pressure drop tests. Four friction factor correlations and six K-factor models are examined.

[†] Advanced Solution of Subchannel Equations in Reactor Thermalhydraulics.

1.1 The ASSERT Subchannel Analysis Code

The ASSERT-IV computer code models transient or steady-state, single- or two-phase flow and heat transfer in rod-bundle fuel channels. It is based on an advanced drift-flux thermal-hydraulic model that accounts for both thermal disequilibrium and the transverse flow found in CANDU^{*}-type fuel channels. The model equations are discretized and solved using a fully implicit procedure. The theory behind the program is fully described in the ASSERT-IV Theory Manual.²

In order to complete ASSERT's system of thermalhydraulic model equations, a number of closure relationships are required. In addition to an equation of state, ASSERT includes constitutive relationships to compute a friction factor, a two-phase friction multiplier, the relative velocity (axial and lateral drift flux), the thermal mixing, the heat transfer to the wall, the interfacial heat transfer, and the critical heat flux. The ASSERT-IV User's Manual¹ explains how these submodels can be controlled using the input data. As this investigation concentrated on the single-phase pressure drop, no CHF calculations are reported.

1.2 The ASSERT Validation Plan

The Stern Laboratories' experiments will be used to perform an extensive validation of the ASSERT code. The pressure drop, void generation, CHF, transient CHF and post-dryout models in ASSERT can all be tested against data from the Stern experiments. Table 1 outlines the validation plan.

Table 1: ASSERT Validation Plan for the Stern Experiments

Year	Validation Study	Stern Tests	ASSERT Models to Validate
'95-'96	Single-Phase Pressure Drop	Pressure Drop, Heat Balance	Channel pressure drop, Friction factor, K-factors (incl. orientation and creep)
'95-'96	Onset-of-Significant Void	Profile Scan	Void generation, Rod temperatures, Pressure drop slope change
'95-'97	Two-Phase Pressure Drop	CHF, Heat Balance	Channel pressure drop, Two-phase multiplier
'95-'97	Critical Heat Flux	CHF	Onset-of-dryout location and power, Bundle orientation and PT creep, CHF look-up table
'96-'97	Transient CHF	Transient	Flow oscillation, Flow ramp
'97-'98	Post-Dryout	Post-Dryout	Post-dryout models

2. Modelling the Single-Phase Pressure Drop Experiments

In this study, the 37-element experiments conducted at Stern Laboratories were simulated with ASSERT. In order to capture the asymmetry of the bundle junction endplates, the full 37-rod bundle must be modelled. A cross-section of the Stern rod bundle, showing all sixty sub-channels, is shown in Figure 1. The bundle geometry and the radial heat flux distribution were taken from Fortman *et al.*³ The axial heat flux and PT creep profiles were provided by Fortman.⁴

^{*} CANada Deuterium Uranium; registered trademark.

The length of the fuel channel was divided into 84 uniformly sized axial nodes, 7 for each of the twelve rod bundles in the channel.

For this study, we used ASSERT-IV, version 2, revision 11, modification level 141, with minor modifications to account for the segmented axial heat flux profile and the friction factor and K-factor models described in this paper.

The friction and form loss models in ASSERT are related to the single-phase pressure drop by

$$\Delta P = \left(f \frac{L}{D} + \sum_i K_i \right) \frac{G^2}{2\rho},$$

where ΔP is the pressure drop over the length of an axial node, f is the friction factor, L is the length of the node, D is the hydraulic diameter, K_i are the form loss coefficients (K-factors) for any bundle appendages in the node, G is the mass flux, and ρ is the density of the fluid. In ASSERT, this equation is applied to each subchannel and axial node in the fuel string.

Since there was only one pressure tap per bundle, only the combined effect of the friction and form losses can be compared to the experimental data of Fortman *et al.*³ To evaluate the separate effects of friction and form, future studies will compare ASSERT predictions to measurements from the single-phase pressure drop experiments, with Bruce 37-element fuel bundles, that were performed at the Sheridan Park Engineering Laboratory (SPEL) by Waters *et al.*⁵ and at the Chalk River Laboratories (CRL) by Hameed.⁶

In this study, four of many possible friction factors and six different form loss models are investigated.

2.1 Friction Factors

The four friction factors used in this study are: (i) the default ASSERT friction factor due to Aly and Groeneveld,⁷ (ii) Hameed's⁶ friction factor, (iii) the Colebrook-White^{8,9} friction factor, and (iv) Selander's¹⁰ friction factor.

The friction factor correlations of Aly and Groeneveld⁷ and Hameed⁶ were both derived from pressure drop measurements in 37-element CANDU fuel bundles, using the Blasius-type equation:

$$f = a Re^b,$$

where a and b are correlation coefficients. These coefficients, and the Reynolds number ranges of the experiments from which they were derived, are listed in Table 2.

Table 2: Blasius-Type Friction Factors

Correlation	a	b	Re Range
Aly & Groeneveld	0.243	-0.216	24,000–42,000
Hameed	0.101	-0.148	152,000–325,000

Although Aly and Groeneveld's correlation was derived from experiments with much smaller Reynolds numbers than the Stern Laboratory tests, it has been successfully applied in the ASSERT models of many experiments covering a wide range of Reynolds numbers.

The Colebrook-White^{8,9} friction factor

$$f = \left[-2 \log \left(\frac{\epsilon/D}{3.7} + \frac{2.51}{\sqrt{f} Re} \right) \right]^{-2}$$

applies to all round tubes (with non-uniform wall roughness) for stable flows with Reynolds numbers greater than about 4000. Since this is an iterative formula, many explicit approximations to it have been derived. Selander¹⁰ recommended

$$f = \left[-2 \log \left(\frac{-4.793}{\text{Re}} \log \left(\frac{10}{\text{Re}} + 0.2 \frac{\epsilon}{D} \right) + 0.2698 \frac{\epsilon}{D} \right) \right]^{-2}.$$

The Colebrook formulae are functions of the relative roughness ϵ/D , which for this study was taken to be a constant value of 0.00012. In later studies, the relative roughness will be calculated by ASSERT based on the given roughness height and the computed hydraulic diameter of the subchannel.

These four friction factors are shown in Figure 2, and their effects on the channel pressure drop are reported in Section 3.2. Note that the two Colebrook formulae are almost coincident. The Blasius-type correlations of Hu¹¹ and Liska,¹² and the Colebrook-Chen^{13,14} formula, will also be examined in a future study.

2.2 Form Loss Models

Form loss coefficients are required to model the increase in pressure drop due to the appendages (junctions/endplates, spacers and bearing pads) of a rod bundle. Three different types of loss coefficients (K-factors) are available to ASSERT users. "Uniform" K-factors (one value for each appendage) are the same in every subchannel; they are usually determined from pressure drop experiments. "Non-uniform" K-factors are specified in the ASSERT input¹ for each subchannel for each appendage type and location. In this study, the set of K-factors is the same for each appendage in the channel. Unlike the other form loss models, the "geometry-based" K-factor model does not use predetermined loss coefficients but calculates the K-factors for each subchannel at each axial node, based on the local flow area and the flow blockage area given in the ASSERT input. This model was developed at CRL¹⁶ to more readily calculate the local K-factors in cases of axial variation in the subchannel geometry, such as pressure tube creep or fuel element strain.

Of the many form loss models available, six were chosen for this study: (i) the uniform K-factors of Hameed,⁶ (ii) Morris *et al.*'s¹⁵ non-uniform K-factors, and geometry-based K-factors determined by (iii) the D'Arcy-Weisbach correlation used by McCracken *et al.*¹⁶ with their geometry data, (iv) Idelchik's⁸ square-edged orifice equation with McCracken's data, (v) Idelchik's orifice equation with Dam's¹⁷ geometry data, and (vi) the orifice equation used by Dam and Lee¹⁸ with Dam's data.

One set of uniform K-factors, determined by Hameed,¹⁹ was designated the reference model. Hameed's values are 0.440 for a bundle junction and 0.112 for a spacer plane. He did not calculate a K-factor for the bearing pad planes, but recommends the value of 0.012 from the Thermalhydraulic Compendium.¹⁴

To model the three bundle orientations (reference R, mirror M and inverted U) in the Stern experiments, a revised set of non-uniform loss coefficients from Morris *et al.*¹⁵ were used. These K-factors were computed using the projected blockage area of each subchannel in one-half of a Bruce 37-element bundle. These values were translated to the three full-bundle orientations of the current simulation. The K-factors for the reference bundle orientation are shown in Figure 3.

Although non-uniform K-factors are sufficient for the different bundle orientations, they cannot account for the change in pressure drop due to pressure tube creep or fuel rod strain. The

original ASSERT geometry-based K-factor model, implemented by McCracken *et al.*,¹⁶ can account for any such change in flow area. This model accepts as input the blocked area of each subchannel, and computes the K-factor using the internal values for flow area and wetted perimeter. This study uses two sets of geometry data and three formulae to compute the loss coefficient.

The original geometry-based K-factor blockage data, first used by McCracken *et al.*,¹⁶ included blockage areas for two planes of bearing pads and one plane of spacers, and an area for the junction that was supposed to account for both the endplate and the area increase at the junction, for the subchannels in one-half of a Bruce 37-element bundle. These values were used to determine the subchannel blockage areas for the bearing pads, spacers and endplates of each orientation of the Stern rod bundle.

The model described by Dam and Lee¹⁸ uses the same formula, but revised area data, to determine a loss coefficient for the increase in flow area at a bundle junction. Applications of Dam and Lee's version of the geometry-based model are described by Dam *et al.*²⁰ and Soulard *et al.*²¹ In the present study, however, the K-factor for a bundle junction is assumed to depend only on the projected blockage area ratio of the subchannel. The more recent geometry data provided by Dam¹⁷ includes the projected blockage areas of each spacer, bearing pad and endplate in each subchannel of one-half of a Stern 37-rod bundle. These values were summed to get the blocked area of each subchannel for the three orientations of the Stern bundle.

In this study, three different formulae are used to calculate the loss coefficient for each subchannel from the blockage data. McCracken *et al.*¹⁶ used the D'Arcy-Weisbach correlation:

$$K = \left[\left(0.6079\varepsilon + 0.1739\varepsilon^2 - 0.3382\varepsilon^3 + 0.5544\varepsilon^4 \right)^{-1} - 1 \right]^2,$$

where

$$\varepsilon = 1 - \frac{A_{\text{blocked}}}{A_{\text{subchannel}}}$$

is the flow area ratio.

Dam and Lee¹⁸ computed the K-factor using an equation from Idelchik²²

$$K = \left[\frac{1}{2}(1 - \varepsilon) + (1 - \varepsilon)^2 + \tau(1 - \varepsilon)^{3/2} \right] / \varepsilon^2$$

for modelling the pressure loss due to a square-edged orifice. They assumed a constant value of 1.1 for the wall thickness coefficient τ .

In the present study, a variation of the above equation:

$$K = \left[\frac{1}{2}(1 - \varepsilon)^{3/4} + (1 - \varepsilon)^2 + \tau(1 - \varepsilon)^{1/8} \right] / \varepsilon^2,$$

from a more recent edition of Idelchik,⁸ was implemented using Idelchik's formula for the wall thickness coefficient:

$$\tau = \left(2.4 - \frac{l}{D_h} \right) \times 10^{-0.25 \frac{0.535(l/D_h)^8}{0.05 + (l/D_h)^7}},$$

where l is the length of the blockage and D_h is the hydraulic diameter of the blocked subchannel.

Figure 4 shows the K-factors for the endplates, bearing pads and spacer plane, using each of the three K-factor formulae above, and the geometry data of McCracken *et al.*¹⁶ Figure 5 shows

the same sets of K-factors using Dam's¹⁷ geometry data. These figures show that the McCracken data produces larger K-factors in the subchannels blocked by endplates or bearing pads, and that the Dam data produces larger K-factors in the subchannels blocked by spacers. The Dam and Lee¹⁸ model based the spacer K-factors on the cross-sectional area of a spacer at any axial location. In the present work, the spacer K-factors are based on the projected blockage area data provided by Dam,¹⁷ resulting in larger loss coefficients for the spacers.

2.3 Test Matrix

The friction and form loss model combinations used in this study are listed in Table 3. The abbreviations are used to indicate these cases in the rest of this paper.

Table 3: Friction and Form Loss Model Test Matrix

Friction Factor	Form Loss Model (Type: Formula/Data)					
	Uniform: Hameed	Non-uniform: Morris	Geometry: D'Arcy-Weisbach/McCracken	Geometry: Idelchik/McCracken	Geometry: Dam & Lee/Dam	Geometry: Idelchik/Dam
Aly and Groeneveld	UH1	NM1	GAM1	GIM1	GCD1	GID1
Hameed	UH2					
Colebrook-White	UH4					
Colebrook-Selander	UH5					

3. Analysis of Results

The heated and unheated single-phase pressure drop tests, from the R1, R2, R3, M, U and C1 test series of the Stern experiments, were simulated using the friction and form loss models listed in Table 3. The computed channel pressure drops were compared to the measured pressure drops, which needed to be interpolated to the fuel channel length. The algebraic mean of the relative difference between the two pressure drops from the points in each test series, and for each friction and form loss model, are summarized in Table 4 for a) the unheated, and b) the heated single-phase pressure drop tests. Since the pressure drop, and thus the loss coefficients, should be lower in a crept pressure tube, the tables show separate averages for the nominal PT cases (the R1, R2, R3, M and U series) and all the test points, including the 3.3% crept PT cases (the C1 series).

Table 4 a): Average Errors for the Unheated Pressure Drop Tests

Series	# Test Points	Friction and Form Loss Model								
		UH1	NM1	GAM1	GIM1	GCD1	GID1	UH2	UH4	UH5
R1	42	1.0%	-19.0%	30.0%	41.9%	10.9%	11.1%	-1.9%	-1.3%	-1.2%
R2	37	5.7%	-14.2%	35.1%	46.8%	15.9%	16.0%	1.1%	1.9%	2.0%
R3	10	5.2%	-13.7%	33.6%	44.8%	15.3%	15.2%	-0.7%	0.5%	0.7%
M	10	6.3%	-13.0%	35.2%	46.6%	16.6%	16.5%	0.7%	1.6%	1.8%
U	40	4.9%	-14.4%	33.8%	45.2%	15.1%	15.1%	-0.1%	0.7%	0.9%
Nominal	139	4.1%	-15.6%	33.1%	44.7%	14.2%	14.2%	-0.3%	0.4%	0.6%
C1	35	12.2%	-14.7%	25.2%	42.8%	9.1%	11.8%	7.4%	8.2%	8.4%
Total	174	5.7%	-15.4%	31.5%	44.3%	13.1%	13.7%	1.2%	2.0%	2.2%

Table 4 b): Average Errors for the Heated Pressure Drop Tests

Series	# Test Points	Friction and Form Loss Model								
		UH1	NM1	GAM1	GIM1	GCD1	GID1	UH2	UH4	UH5
R1	22	2.1%	-18.8%	32.4%	44.9%	12.3%	12.6%	0.8%	0.8%	0.9%
R2	13	3.1%	-18.6%	34.1%	47.1%	13.4%	13.8%	2.4%	2.6%	2.7%
R3	4	3.0%	-18.1%	33.6%	46.2%	13.3%	13.6%	1.6%	1.6%	1.7%
M	4	2.3%	-19.0%	33.0%	45.8%	12.5%	12.9%	1.4%	1.6%	1.7%
U	11	1.6%	-19.5%	32.0%	44.6%	11.8%	12.1%	0.6%	0.8%	0.8%
Nominal	54	2.3%	-18.8%	32.8%	45.5%	12.6%	12.9%	1.2%	1.4%	1.5%
C1	34	10.1%	-18.8%	24.1%	43.2%	6.7%	9.8%	9.2%	9.5%	9.6%
Total	88	5.4%	-18.8%	29.5%	44.6%	10.3%	11.7%	4.3%	4.5%	4.6%

The computed and measured pressure drops are also compared in Figures 6 and 7 for the unheated and heated single-phase tests, respectively. The tables and figures show that the choice of friction factor has a much smaller effect on the overall pressure drop than the choice of the form loss model and its associated data.

3.1 Effect of the Form Loss Model on the Channel Pressure Drop

The closest agreement with the experimental pressure drop was obtained using the uniform K-factor model of Hameed¹⁹ (the UH# models in Table 4), which predicted the pressure drops to within -2 to 6% of the experimental pressure drops over a nominal fuel channel (R1, R2, R3, M, and U series). As noted by Balint,²³ the R1 series channel pressure drop is slightly lower than for the other series, and the UH# models predict the R1 pressure drop to within $\pm 2\%$.

As expected, the pressure drop is overpredicted for the crept PT cases (the C1 series), since the increase in flow area and redistribution of the flow lower the pressure drop and reduce the bundle-averaged loss coefficient. Hameed has planned more experiments using crept fuel channels, which will provide more K-factors as a function of the pressure tube creep.

Using the non-uniform K-factors of Morris *et al.*¹⁵ (the NM1 model), the pressure drop is underpredicted by 13 to 19 percent, for both the nominal and crept PT cases. These K-factors are not recommended for analysis of the Stern Laboratories' experiments.

Using a geometry-based K-factor model with McCracken's¹⁶ data, the pressure drop is overpredicted by 30–35% using the D'Arcy-Weisbach correlation (the GAM1 model) with a nominal PT and 23–25% with a crept PT, and by 42–47% and 43–46%, respectively, using the Idelchik⁸ formula (the GIM1 model). Since the endplate loss factors are too large, McCracken's geometry data are not suitable for analysis of the Stern experiments.

Using a geometry-based K-factor model with Dam's¹⁷ data, the pressure drop is overpredicted by 11–16% using either orifice equation with a nominal PT, and by 7–9% using Dam and Lee's¹⁸ formula (the GCD1 model) and 10–12% using the Idelchik⁸ formula (the GID1 model) with a crept PT. This is close enough to warrant further examination of this model. Part of the overprediction is due to the use of Aly and Groeneveld's⁷ friction factor, and part is surely due to the excessively large spacer K-factors (shown in Figure 5). With revised spacer geometry data and Hameed's or a Colebrook friction factor, the predictions should be much better.

3.2 Effect of the Friction Factor on the Channel Pressure Drop

Table 4 and Figures 6 and 7 show that the friction factor of Aly and Groeneveld⁷ produces higher channel pressure drops than Hameed's correlation or the Colebrook formulae. Comparing

the pressure drops from the nominal PT cases using Hameed's¹⁹ uniform K-factors, Aly and Groeneveld's correlation (the UH1 model in Table 4) overpredicts the pressure drop by 1–6%, Hameed's correlation (UH2) is accurate to within 2%, and the Colebrook formulae (UH4 and UH5) are within -1% and 3%.

With Hameed's uniform K-factors on a nominal (uncrept) fuel channel, therefore, either Hameed's friction factor correlation or the Colebrook formulae produce channel pressure drops in excellent agreement with the experimental data. Further testing is required to evaluate these friction factors along with the geometry-based K-factor models on both nominal and crept PT cases. The implementation of the Colebrook friction factor models can be refined by having ASSERT compute the relative roughness for each subchannel from the roughness height (which in the Stern experiment is different for the fuel rods and the PT ceramic liner) and the hydraulic diameter (which varies between subchannels).

3.3 Axial Pressure Drop Profiles

Examples of the cumulative axial pressure drop profiles are shown in Figures 8 and 9, each showing the computed and measured pressure drop profiles for a range of flow rates. In these figures, the unconnected symbols represent the pressure computed by ASSERT at each axial node (seven per 50 cm bundle), and the symbols connected by the straight lines represent the measured pressures (one near the centre of each bundle). The pressure drops shown are relative to the reference pressure at the end of the twelve-bundle fuel channel.

Figure 8 shows the pressure drops using Aly and Groeneveld's⁷ friction factor and Hameed's¹⁹ uniform K-factors (the UH1 model), for a series of test cases in the reference orientation, at an exit pressure of 9 MPa, an inlet temperature of 270°C, and zero heat flux. The pressure drop profiles predicted by ASSERT are in excellent agreement with the experimental data for these cases.

Figure 9 shows pressure drop profiles using the geometry-based K-factor model with Dam's¹⁷ data and the Dam and Lee¹⁸ formula (the GCD1 model), for two 3.3% crept PT cases at an exit pressure of 9 MPa, an inlet temperature of 250°C, and a power of 3.0 MW. For these cases, the agreement is also reasonably good.

4. Conclusions and Recommendations

The results presented here are subject to consideration of the uncertainties in the measurements of the experimental pressure drop data, geometry and boundary conditions, as well as the ASSERT pressure drop submodels and their associated coefficients and data. The validation of ASSERT for single-phase pressure drop in CANDU fuel channels is ongoing.

The best agreement between the computed and measured channel pressure drops was obtained using the uniform K-factors of Hameed. Using the non-uniform K-factors of Morris *et al.*, the pressure drop was significantly underpredicted, and using the geometry-based K-factor model with McCracken's data the pressure drop was greatly overpredicted. Using geometry-based K-factors based on Dam's data, the pressure drop was moderately overpredicted. The spacer geometry data provided by Dam should be reviewed.

The choice of friction factor made only a small difference to the pressure drop, but Hameed's correlation was slightly better than the two Colebrook formulae, which were better than Aly and Groeneveld's correlation. The analysis needs to be performed again using the

Colebrook formulae with the relative roughness calculated separately for each subchannel, to account for variations in the roughness height and the hydraulic diameter.

Before more validation against the Stern Laboratory data is performed, the separate effects of the friction and form losses in ASSERT should be compared with the single-phase pressure drop experiments performed at SPEL and by Hameed, from which the friction factor and the junction and spacer K-factors can be derived.

For future applications of ASSERT, where matching the experimental pressure drop is the primary concern, we recommend using uniform K-factors determined from experiments with similar bundle and pressure tube geometries. For most applications of ASSERT, however, when it is important to capture the local flow patterns and phase distribution (as when predicting the initial dryout location or the effect of PT creep), we recommend using the geometry-based K-factor model with revised data and Idelchik's thick-edged orifice equation. Hameed's friction factor and both Colebrook friction factors are recommended, pending further examination of the Colebrook friction factors with locally computed relative roughness factors.

The results and conclusions presented here are preliminary as the implementation of the Colebrook friction factor correlations and the geometry-based K-factor model require further review. The validation of ASSERT against the single-phase pressure drop data from Stern Laboratories is ongoing.

5. Acknowledgements

The development of ASSERT and the work described here was funded by the CANDU Owners Group (COG) Fuel Channel Critical Power (FCCP) Working Party.

The authors gratefully acknowledge the prompt reviews of this paper by T. Balint, J. MacKinnon and I. Cheng of Ontario Hydro and by R. Dam of AECL (Sheridan Park).

6. References

1. J.C. Kiteley, M.B. Carver, A. Banas, D.S. Rowe and J.F. Wasilewicz, "ASSERT-IV (Version 2) User's Manual," unpublished AECL report, 1991.
2. M.B. Carver, J.C. Kiteley, A. Banas, A. Tahir and D.S. Rowe, "ASSERT-IV (Version 2) Theory Manual," unpublished AECL report, 1988.
3. R.A. Fortman, R.C. Hayes and G.I. Hadeller, "37-Element CHF Program: Phase 1 Test Results," unpublished Stern Laboratories report, 1994.
4. R.A. Fortman, letter to J.C. Kiteley, January 1995.
5. W.F. Waters, B.M. Pearson and J.P. Norrie, "Experimental Determination of K-Values for CANDEV Fuel Bundles," unpublished AECL report, 1986.
6. A. Hameed, "Pressure Drop Measurements on Bruce-Type 37-Element CANDU Fuel Bundles in Freon: Phase I Aligned Bundles," unpublished AECL report, 1995.
7. A.M.M. Aly and D.C. Groeneveld, "Detailed Axial Pressure Drop Measurements for 37-Element Bundles: 1. Single Phase Flow," unpublished AECL report, 1979.
8. I.E. Idelchik, "Handbook of Hydraulic Resistance," 3rd Edition, CRC Press Inc., 1994.

9. F.M. White, "Fluid Mechanics," 2nd Edition, McGraw-Hill Book Company, 1986.
10. W.N. Selander, "Explicit Formulas for the Computation of Friction Factors in Turbulent Pipe Flow," AECL-6354, November 1978.
11. R.H. Hu, "Pressure Drop of Coolant Flow Through Bruce Fuel Bundles," unpublished report, 1974.
12. M. Liska, "CANDU-600 Reactor Fuel Channel Components: Hydraulic Losses," unpublished AECL report, 1982.
13. N.H. Chen, "An Explicit Equation for Friction Factor in Pipe," *Ind. Eng. Chem. Fund.*, Vol. 18, pp. 296-297, 1979.
14. D.C. Groeneveld and L. K.H. Leung, "Compendium of Thermalhydraulic Correlations and Fluid Properties," unpublished AECL report, 1990.
15. R.J. Morris, M.B. Carver and J.C. Kiteley, "Calculation of Flow Loss Factors for CANDU 37-Element Bundle Appendages," unpublished AECL report, 1989.
16. I.K. McCracken, J.C. Kiteley and M.B. Carver, "ASSERT Modelling of Pressure Drop Across Bruce Bundle Appendages (Single Phase Flow)," unpublished AECL report, 1991.
17. R. Dam, personal communication with J.C. Kiteley, March 1995.
18. R. Dam and N. Lee, "Commissioning of ASSERT-IV for CCP Calculations in CANDU 6 Pressure Tubes," unpublished AECL report, 1994.
19. A. Hameed, communication to COG WP #7 (FCCP), August 1995.
20. R.F. Dam, J.C. Kiteley, M.R. Soulard, M.B. Carver, K.F. Hau, G. Hotte and P.D. Thompson, "ASSERT/NUCIRC Commissioning for CANDU 6 Fuel Channel CCP Analysis," 1994 CNS Nuclear Simulation Symposium, Pembroke, Ontario, October 1994.
21. M.R. Soulard, R.F. Dam, M.B. Carver, J.C. Kiteley, G. Hotte and R.A. Gibb, "Investigation into the Modelling of the Effect of Pressure Tube Creep on CHF, Dryout Power and Pressure Drop," 1995 CNA/CNS Conference, Saskatoon, Saskatchewan, June 1995.
22. I.E. Idelchik, "Handbook of Hydraulic Resistance," 2nd Edition, CRC Press Inc., 1986.
23. T. Balint, "Single-Phase and Two-Phase Pressure Drop Methodology for 37-Element Uncrept Fuel," unpublished Ontario Hydro report, 1995.

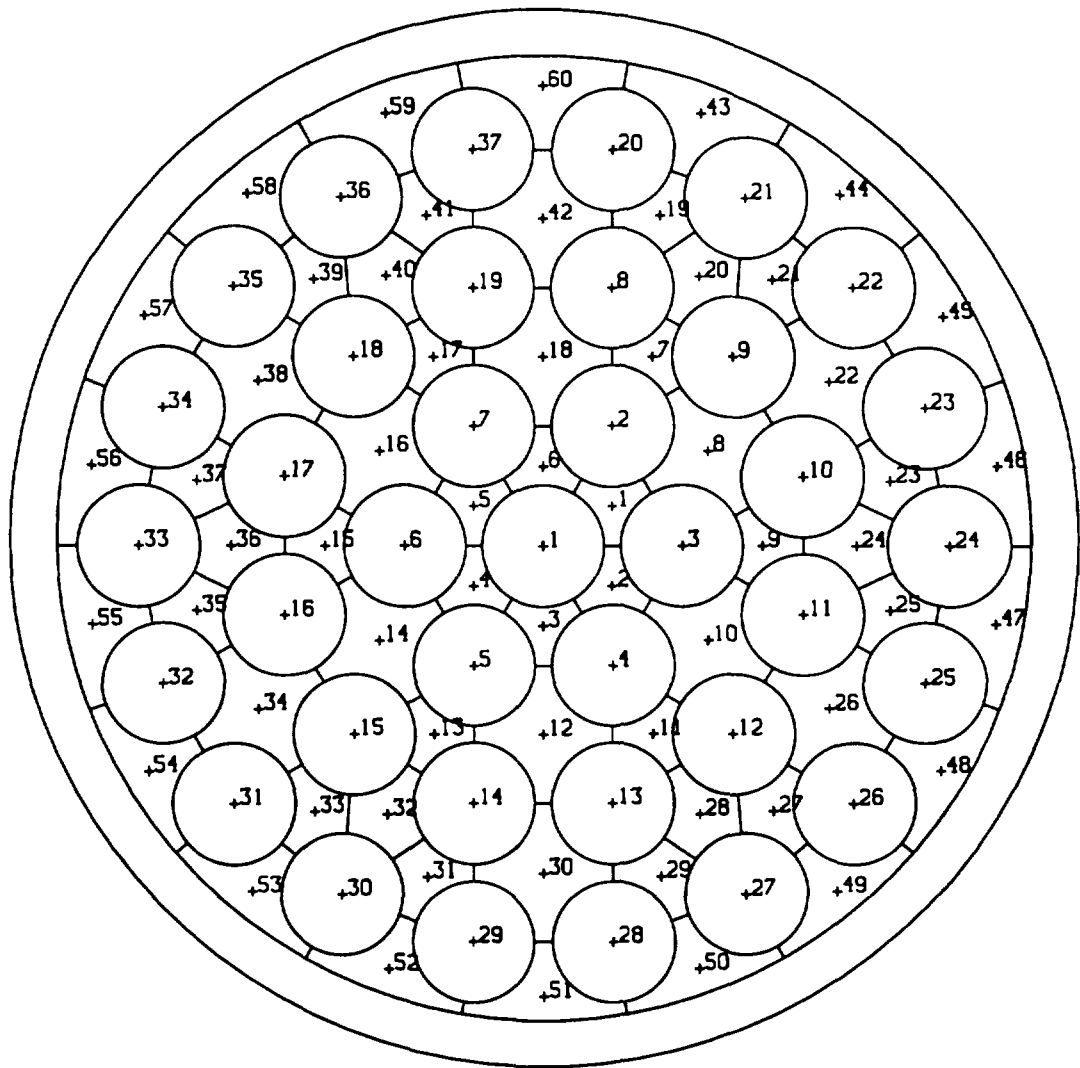


Figure 1: ASSERT Model of the Stern Rod Bundle

Cross-section of a nominal fuel channel showing the 37 fuel elements and the 60 subchannels used in the ASSERT model.

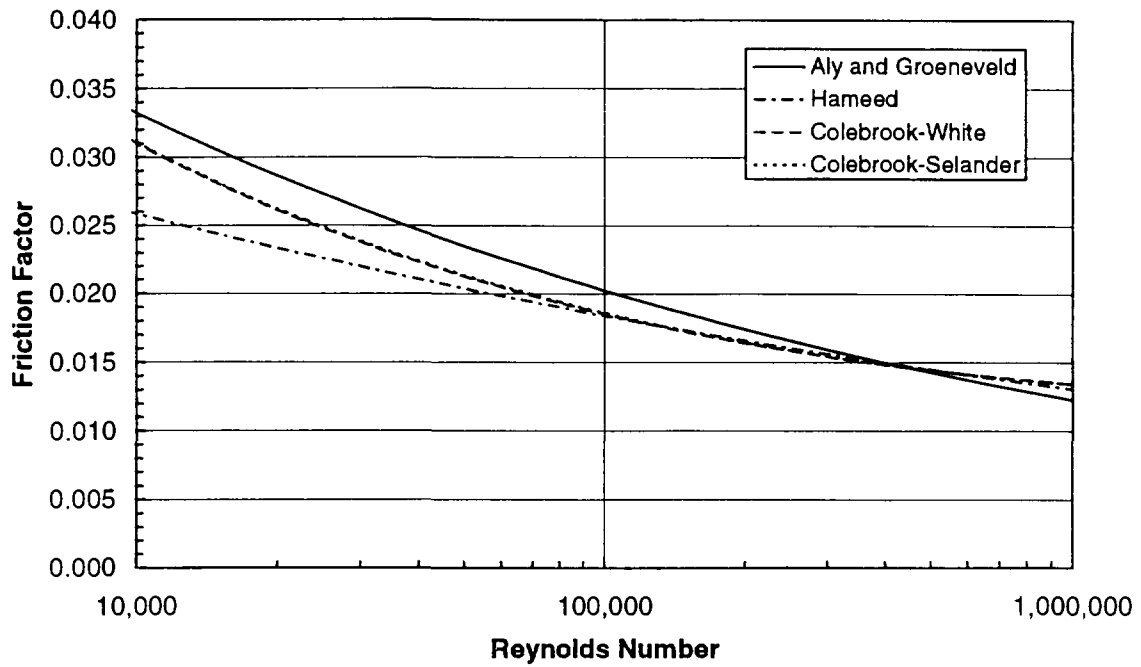


Figure 2: Friction Factors

Comparison of the turbulent friction factors of Aly and Groeneveld,⁷ Hameed,⁶ Colebrook⁸ and Selander.¹⁰

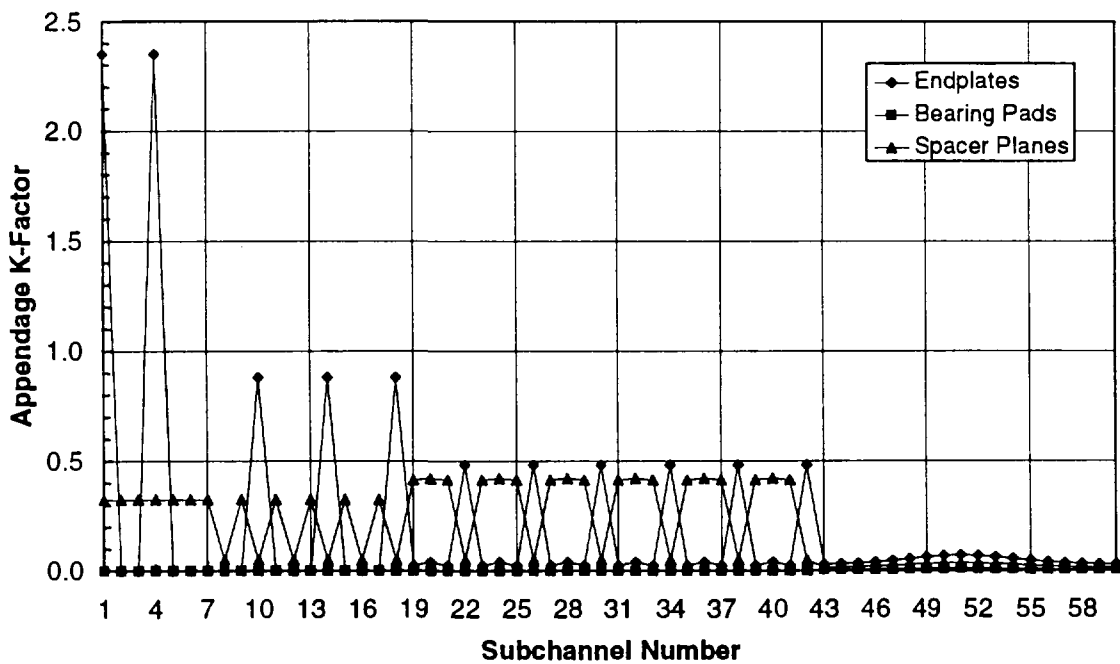


Figure 3: Appendage Loss Coefficients of Morris *et al.*

The K-factors for the endplate, bearing pads and spacers for each subchannel, for a bundle in the reference orientation, based on the coefficients determined by Morris *et al.*¹⁵

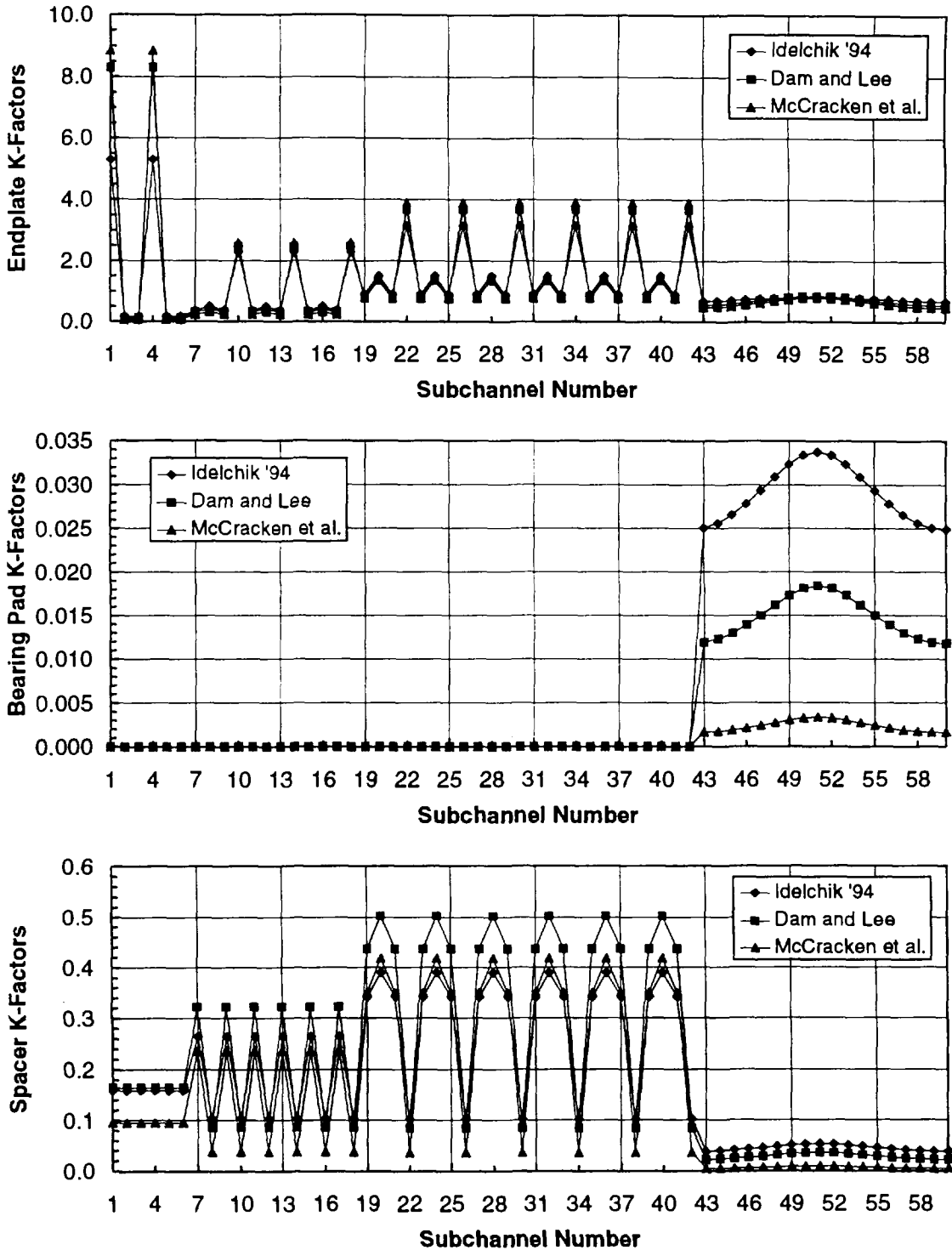


Figure 4: Appendage Loss Coefficients Using the McCracken Data

The geometry-based K-factors for the a) endplates (of a bundle in the reference orientation), b) bearing pads and c) spacers for each subchannel in a nominal PT, using the geometry data of McCracken *et al.*¹⁶ and the formulae of McCracken *et al.*,¹⁶ Dam and Lee¹⁸ and Idelchik.⁸

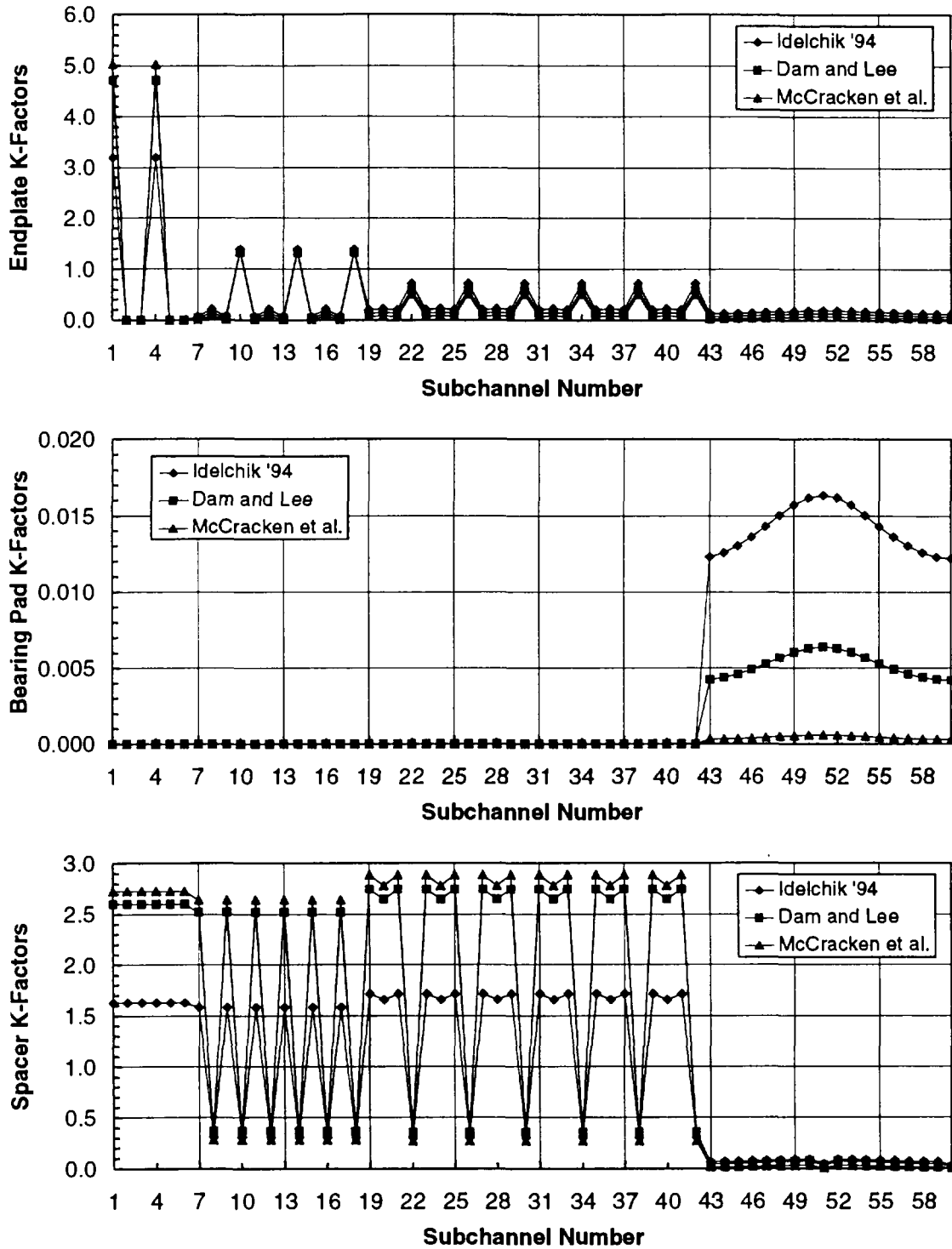


Figure 5: Appendage Loss Coefficients Using the Dam Data

The geometry-based K-factors for the a) endplates (in the reference orientation), b) bearing pads and c) spacers for each subchannel in a nominal PT, using the geometry data of Dam¹⁷ and the formulae of McCracken *et al.*,¹⁶ Dam and Lee¹⁸ and Idelchik.⁸

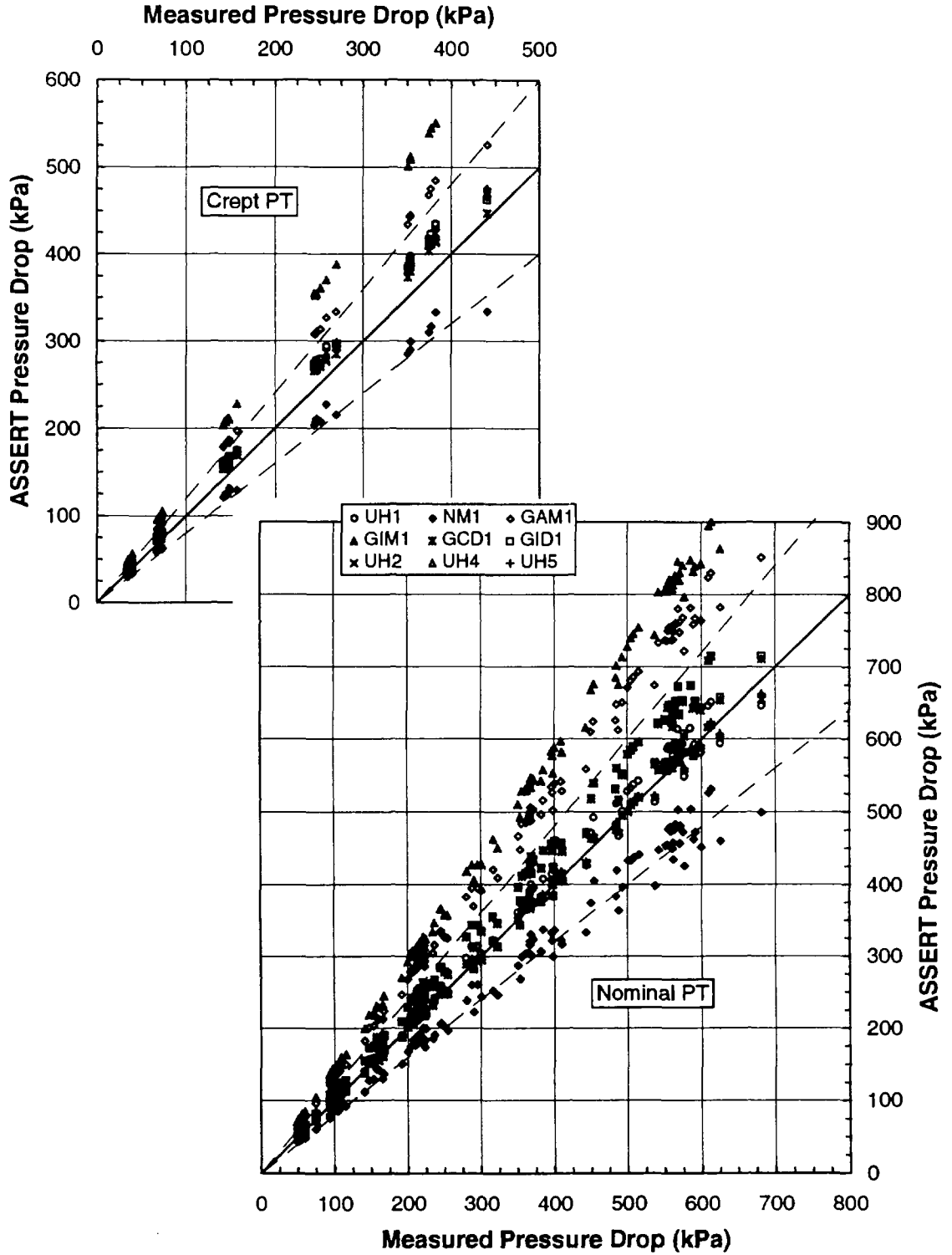


Figure 6: Comparison of Predicted and Measured Channel Pressure Drops (Unheated)
 The predicted channel pressure drop is compared to the measured pressure drop, for the unheated cases with a nominal (bottom) or crept (top) PT, using each friction and form loss model.

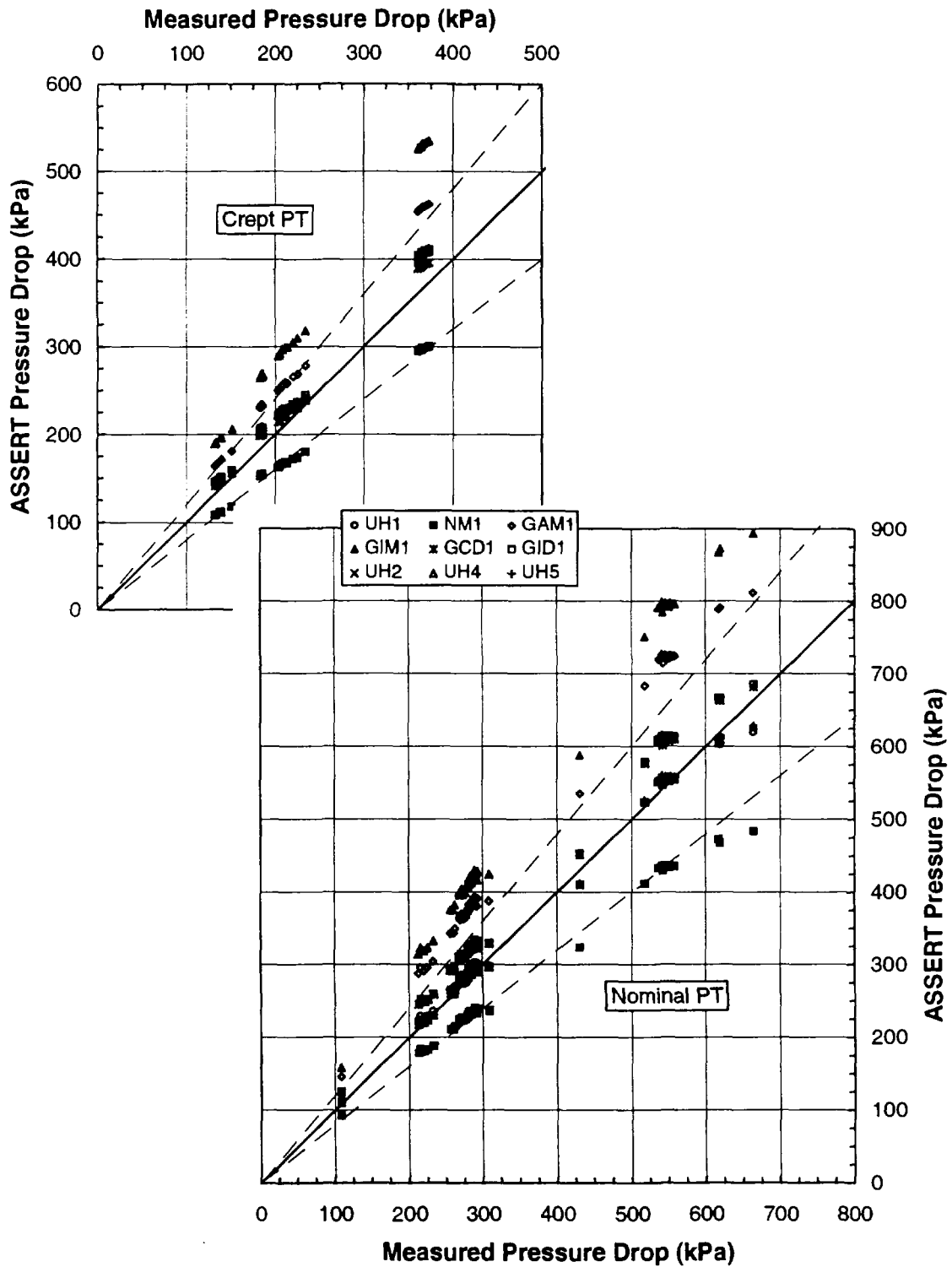


Figure 7: Comparison of Predicted and Measured Channel Pressure Drops (Heated)

The predicted channel pressure drop is compared to the measured pressure drop, for the heated cases with a nominal (bottom) or crept (top) PT, using each friction and form loss model.

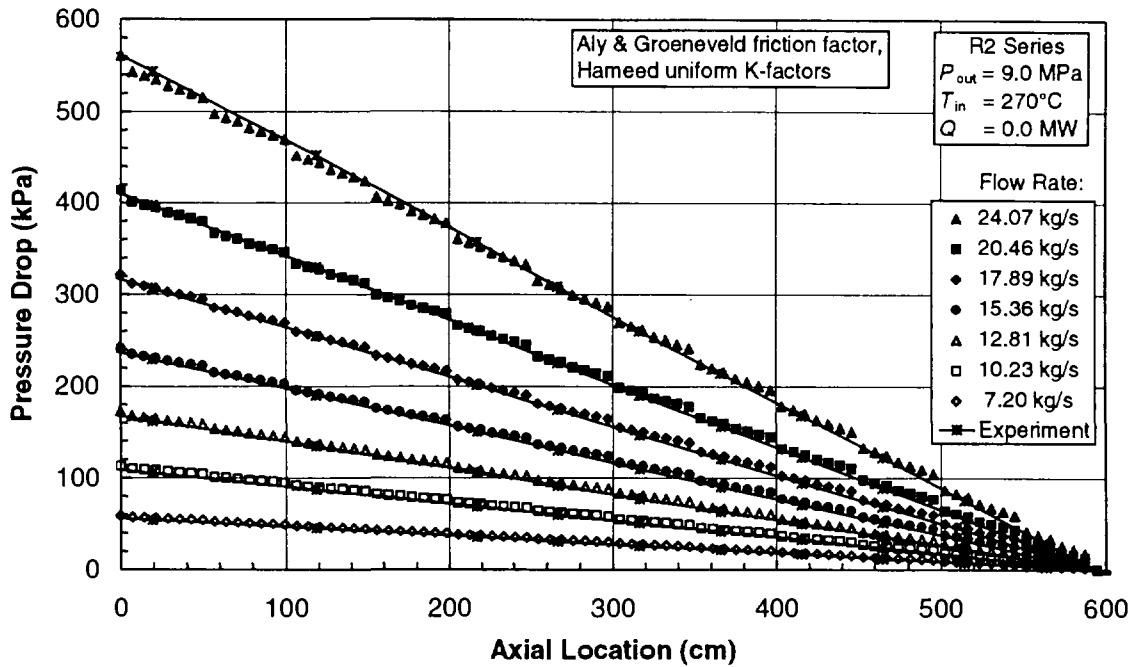


Figure 8: Pressure Drop Profiles for Unheated, Nominal PT Cases

Predicted and measured axial pressure drop profiles for several unheated, nominal PT cases, using Aly and Groeneveld's⁷ friction factor and Hameed's¹⁹ uniform K-factors.

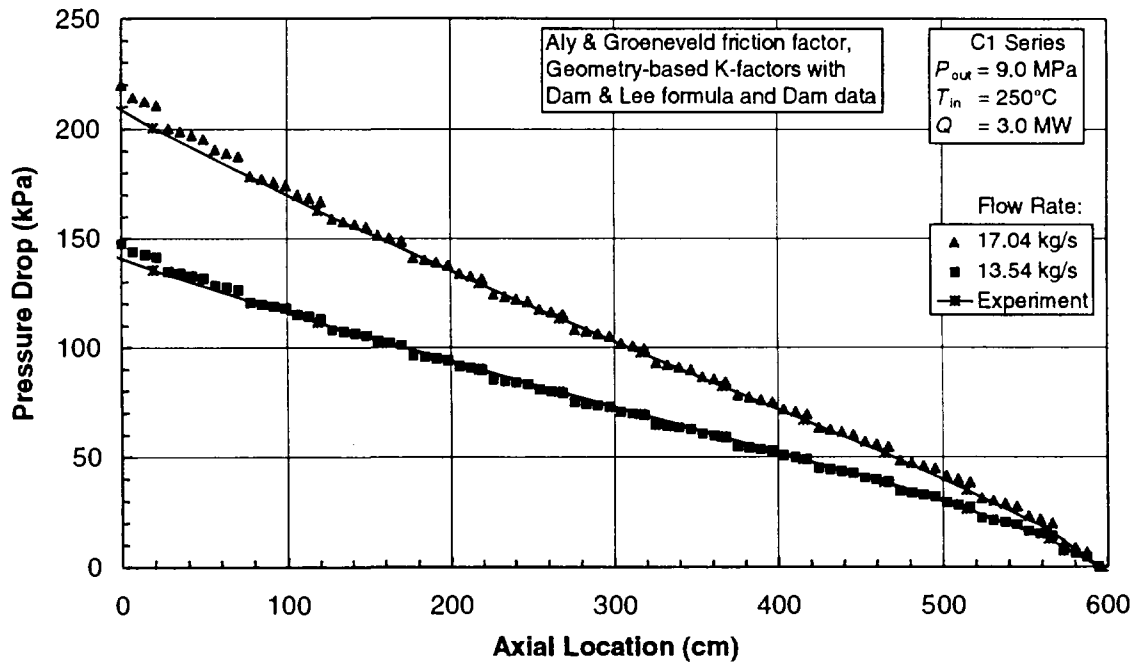


Figure 9: Pressure Drop Profiles for Heated, Crept PT Cases

Pressure drop profiles for several heated, crept PT cases, using Aly and Groeneveld's⁷ friction factor and the geometry-based K-factor model with Dam's¹⁷ data and Dam and Lee's¹⁸ formula.